J Physiol (2003), **546.2**, *pp.* 511–520

DOI: 10.1113/jphysiol.2002.026070
www.jphysiol.org

Journal of Physiology

Chick hair cells do not exhibit voltage-dependent somatic motility

David Z. Z. He *, Kirk W. Beisel †, Lin Chen ‡, Da-Lian Ding ‡, Shuping Jia *, Bernd Fritzsch § and Richard Salvi ‡

* *Hair Cell Biophysics Laboratory and † Department of Genetics, Boys Town National Research Hospital, Omaha, NE, ‡ Hearing Research Laboratory, University of Buffalo, NY and § Department of Biomedical Sciences, Creighton University, Omaha, NE, USA*

It is generally believed that mechanical amplification by cochlear hair cells is necessary to enhance the sensitivity and frequency selectivity of hearing. In the mammalian ear, the basis of cochlear amplification is believed to be the voltage-dependent electromotility of outer hair cells (OHCs). The avian basilar papilla contains tall and short hair cells, with the former being comparable to inner hair cells, and the latter comparable to OHCs, based on their innervation patterns. In this study, we sought evidence for somatic electromotility by direct measurements of voltage-dependent length changes in both tall and short hair cells at nanometre resolution. Microchamber and whole-cell voltage-clamp techniques were used. Motility was measured with a photodiode-based measurement system. Non-linear capacitance, an electrical signature of somatic motility, was also measured to complement motility measurement. Significantly, chick hair cells did not exhibit somatic motility nor express non-linear capacitance. The lack of somatic motility suggests that in avian hair cells the active process resides elsewhere, most likely in the hair cell stereocilia.

(Received 17 June 2002; accepted after revision 25 October 2002; first published online 29 November 2002)
Corresponding author D. Z. Z. He: Hair Cell Biophysics Laboratory, Boys Town National Research Hospital, 555 North 30th Street, Omaha, NE 68131, USA. Email: hed@boystown.org

The cochlear amplifier is the name given to processes that provide mechanical amplification of low-level signals in the inner ear. This amplification is presumably responsible for the ear's extraordinary sensitivity and frequency selectivity as well as the production of spontaneous, acoustic and electrically evoked otoacoustic emissions (for reviews see Brownell, 1990; Dallos, 1996; Hudspeth, 1997). In mammals, the basis of cochlear amplification is believed to be the voltage-dependent somatic length change (termed electromotility) of OHCs (Brownell *et al.* 1985). It has been proposed that the motor candidate is a membrane-bound voltage-sensitive molecule or assembly of molecules (Holley & Ashmore, 1988; Dallos *et al.* 1991) able to change area when the membrane potential changes (Iwasa, 1994). Morphological studies have shown that large protein particles (~10 nm in diameter) with packing densities possibly exceeding 5100 μm^{-2}, cover as much as 75 % of the plasma membrane (Forge, 1991). Recently, the gene named prestin that codes the motor protein was identified (Zheng *et al.* 2000).

Amphibian and reptilian ears are also sensitive, sharply tuned and produce otoacoustic emissions despite the fact that they lack OHCs (for review see Manley *et al.* 2000). Nevertheless, amphibians spontaneously emit sounds from their ears that can be modulated by current injected into the inner ear (Wit *et al.* 1989). Furthermore, current injected into lizard ears generated otoacoustic emissions that could be modulated by acoustic stimulation (Manley *et al.* 2001). These results are consistent with a cochlear amplifier in which the stereocilia not only act as a receptor organelle, but also as a force-generator (for reviews see Hudspeth, 1997; Fettiplace *et al.* 2001). Indeed, active hair-bundle motion has been observed in hair cells of turtles and bullfrogs in response to voltage changes (Crawford & Fettiplace, 1985; Howard & Hudspeth, 1987; Martin & Hudspeth, 1999; Ricci *et al.* 2000, 2002).

Avian hearing is intermediate in range between that of reptiles and mammals. There are two types of hair cells in the chick inner ear (Tanaka & Smith, 1979), the tall hair cell (THC) and the short hair cell (SHC). Like mammals, there appears to be a division of labour between THCs and SHCs with the former receiving predominantly afferent innervation and the latter receiving efferent innervation (Fischer, 1994). The characteristics and the innervation pattern of THCs and SHCs suggest that they are analogous to the inner and outer hair cells, respectively, of the mammalian cochlea. Chick ears produce robust distortion products and spontaneous otoacoustic emissions that disappear when the hair cells are destroyed and which recover when the hair cells regenerate (Chen *et al.* 1996). One compelling result that suggests the existence of an electro-mechanical feedback process (also known as reverse transduction) in the chick cochlea is the production of electrically evoked otoacoustic emissions

that decrease in amplitude with hair cell loss (Chen *et al.* 2001). It has been suggested that, by analogy with mammalian OHCs, SHCs may perform a motor function supplying tuned energy into the vibration of the cochlear partition (for review see Fettiplace & Fuchs, 1999). Indeed, spontaneous as well as evoked damped oscillatory bundle movements have been observed in chick SHCs (Hudspeth *et al.* 2000). It remains equivocal, however, whether chick short hair cells also possess somatic motility, which could also contribute to the active process. In this study, we attempted to determine whether SHCs exhibited electromotility by measuring somatic length change with a photodiode-based measurement system, and by measuring non-linear capacitance, a gating charge movement arising from a redistribution of charged voltage sensors across the membrane (Ashmore, 1989; Santos-Sacchi, 1991). The non-linear capacitance has widely been used as a signature of the electromotility process in cochlear outer hair cells (Santos-Sacchi, 1991; Gale & Ashmore, 1997*a*; Zheng *et al.* 2000).

METHODS

Care and use of the animals in this study were approved by NIH grants and the Animal Care and Use Committee of the Boys Town National Research Hospital, USA.

Hair cell preparation

Dissection of chick hair cells followed the description given by Fuchs *et al.* (1988). In brief, chicks (Leghorns, 2–3 weeks post-hatch) were decapitated following a lethal dose of sodium pentobarbital (200 mg kg^{-1}, I.P.). The skull was split along the sagittal midline. Basilar papillae were dissected out via a medial approach in Leibovitz L-15 medium (supplemented with 15 mM Hepes and adjusted to pH 7.3, 300 mosmol l^{-1}). After the basilar papillae were extracted, the tegmentum vasculosum was removed using forceps. To obtain dissociated hair cells, the basilar papillae were transferred to enzymatic medium which contained 1 ml L-15 and 1 mg collagenase type IV (Sigma). After 15 min incubation at room temperature (23 ± 2 °C), the epithelium was transferred to the experimental bath containing fresh L-15 medium with fetal bovine serum (1 % in volume). Solitary hair cells were obtained with gentle trituration of the tissue with a small pipette.

Adult gerbils were decapitated following a lethal dose of sodium pentobarbital (200 mg kg^{-1}). A detailed description of dissection of gerbil OHCs is given elsewhere (He *et al.* 1994).

Microchamber technique

A detailed description of our motility measurement technique is given elsewhere (Evans *et al.* 1991; He *et al.* 1994). In brief, a suction pipette or microchamber was used to mechanically hold the cell and to deliver voltage commands. Microchambers were fabricated from 2 mm thin-walled glass tubing (A-M Systems, Inc., Carlsborg, WA, USA) by a Flaming/Brown micropipette puller (Model P-87; Sutter Instrument Company, Novato, CA, USA) and heat-polished to an aperture diameter close to that of a chick hair cell (about 8 μm). The microchamber, with a series resistance of approximately 0.5–0.6 MΩ, was mounted in an electrode holder, which was held by a Leitz 3-D micromanipulator (Leitz, Germany). By moving the microchamber, cells in the bath could be picked up easily. The experimental bath, which contained the solitary hair cells, was placed on the stage of an upright microscope (Leica DM LB; Leica Microsystems, Inc., NY, USA). The bath was grounded via a Ag/AgCl electrode. The microchamber was connected to the voltage command generator by a Ag/AgCl wire. The suction port of the microchamber holder was connected to a micrometer-driven syringe to provide positive or negative pressure in order to draw in or expel the cells. The inserted cell and the microchamber formed a resistive seal (3–4 MΩ) that was mechanically stable.

Motility measurement

Motility was measured and calibrated by a photodiode-based measurement system mounted on the Leica microscope. After the cell was inserted into the microchamber (Fig. 2*A*) or after whole-cell voltage-clamp configuration was established (Fig. 2*B*), the magnified image of the edge of the cuticular plate was projected onto a photodiode through a rectangular slit. The image seen by the photodiode was also monitored by a CCD Sony video camera through a beam splitter. The position of the slit in front of the photodiode was adjustable so that the image of the cuticular plate could always be projected onto the photodiode without moving the cell. Somatic length changes, evoked by voltage stimuli, modulated the light influx to the photodiode when the moving object (magnified edge of the cuticular plate) was projected onto the photodiode through the slit. The photocurrent response was calibrated to displacement units by moving the slit a fixed distance (0.5 μm) with the image of the cell in front of the photodiode. After amplification, the photocurrent signal was low-pass filtered by an anti-aliasing filter before being digitized by a Metrabyte DAS-16F data acquisition board (Keithley Instruments, Taunton, MA, USA) in an IBM-compatible computer. The photodiode system had a cutoff (3 dB) frequency of 1100 Hz. The sampling frequency was 5 kHz. In general, an average of 50 presentations was preset for each trial. With an averaging of 50 trials and low-pass filtering set at 1 kHz, movement amplitudes as low as 5 nm could be detected for either the microchamber or whole-cell voltage-clamp techniques. While most experiments were done with the optical/photodiode system that had 5 nm resolution, some motility measurements were made with a photodiode/optical system that had a resolution of 10 nm. The electrical stimulus was a sinusoidal voltage burst of 120 or 240 mV (peak-to-peak) and 200 ms duration for the microchamber technique. In most experiments, 100 Hz was chosen, although in some cases, 250 and 1000 Hz were also used. The stimuli were generated by a programmable stimulus generator (Quatech, Inc., Akron, OH, USA) in an IBM-PC-compatible computer. When motility was measured using the whole-cell voltage-clamp technique, step stimuli were used. The photocurrent signal was low-pass filtered at 1000 Hz before being digitized by a 16-bit A–D board (Digidata 1322A, Axon Instruments, Inc.).

Whole-cell voltage-clamp and non-linear capacitance measurements

Whole-cell voltage-clamp recordings were performed on the Leica microscope and with an Axopatch 200B amplifier (Axon Instruments). The patch pipette with the headstage was held by a Narishige 3-D micromanipulator (MHW-3; Narishige International USA, Inc., NY, USA). Whole-cell voltage-clamp tight-seal recordings were established as described by Fuchs *et al.* (1988) for chick hair cells. The patch electrodes were pulled from 1.5 mm glass capillaries (A-M Systems) using a Flaming/Brown Micropipette Puller (Model P-87; Sutter Instrument Co.). Recording pipettes had open tip resistances of 4–5 MΩ and were filled with an internal solution that consisted of (mM): 140 KCl,

2 $MgCl_2$, 10 EGTA and 10 Hepes, KOH was used to adjust pH to 7.3. The access resistance typically ranged from 6 to 15 MΩ after the whole-cell recording configuration was established. Approximately 70–75 % of the series resistance was compensated.

Voltage steps applied to hair cells generated both ionic and capacitive currents. To measure non-linear capacitive currents, the following composition of intracellular and extracellular media was used to isolate capacitive currents by blocking K^+ and Ca^{2+} currents. The internal solution consisted of (mM): 140 CsCl, 2 $MgCl_2$, 10 EGTA, and 10 Hepes at pH 7.3. CsOH was used for pH adjustment. The external solution contained (mM): 120 NaCl, 20 TEA-Cl, 2 $CoCl_2$, 2 $MgCl_2$, 10 Hepes and 5 glucose at pH 7.3. NaOH was used for pH adjustment. The osmolarity was adjusted to 300 mosmol l^{-1} for all solutions used in this study. Two protocols were used to obtain motility-related gating charge movement and the corresponding non-linear membrane capacitance. First, a standard *P*/−4 linear subtraction procedure was used. Voltage-dependent capacitive currents were extracted after the voltage-independent fraction of the membrane capacitance was subtracted using a standard *P*/−4 linear subtraction procedure (Bezanilla & Armstrong, 1977). This technique derives non-linear charge movement from total charge movement by subtracting estimates of linear charge movement obtained at a membrane potential where non-linear components are small or absent. With this protocol, the cells were held and subtracted at −120 mV. Voltage steps in 10 ms duration varied between −120 and 10 mV. Secondly, evaluation of membrane capacitance was made at different potentials by transient analysis of currents evoked by a voltage stair step stimulus. The technique has been described in detail elsewhere (Huang & Santos-Sacchi, 1993). Briefly, the cell was stimulated with stair voltage command between −130 mV and +40 mV in increments of 10 mV from a holding potential of −70 mV. The duration of each step was 10 ms. From each step response, membrane capacitance (C_m) and resistance (R_m) and serial resistance (R_s) were calculated as a function of membrane voltage. C_m has a linear component, which is a function of the total cell membrane area, and a non-linear component, which is a measure of the charge movement of the motility voltage sensor. The non-linear capacitance can be described as the first derivative of a two-state Boltzmann function relating non-linear charge movement to voltage (Ashmore, 1989; Santos-Sacchi, 1991). The capacitance function is described as:

$$C_m = \frac{Q_{max}\alpha}{\exp[\alpha(V_m - V_{½})]\{1 + \exp[-\alpha(V_m - V_{½})]\}^2} + C_{lin},$$

where Q_{max} is maximum charge transfer, $V_{1/2}$ is the voltage at which the maximum charge is equally distributed across the membrane, C_{lin} is linear capacitance, and $\alpha = ze/kT$ is the slope factor of the voltage dependence of charge transfer where k is Boltzmann's constant, T is absolute temperature, z is valence and e is electron charge. Capacitive currents were filtered at 5 kHz and digitized at 10 kHz using pClamp 8.0 software (Axon Instruments), running on an IBM-compatible computer and a 16-bit A/D converter (Digidata 1322A, Axon Instruments).

RESULTS

Measurements of somatic motility of chick hair cells

Our selection of THCs and SHCs followed from the definition of tall and short hair cells established by Tanaka & Smith (1978) according to their differences in morphology, position and innervation. Accordingly, THCs have a length greater than the width of the cuticular plate; for SHCs the width of the apical surface is greater than their length. Whole-cell voltage-clamp recordings also indicate that SHCs and THCs possess different membrane conductances (for review, see Fuchs, 1992). We first used the microchamber technique to measure motility. This technique was relatively easy and more importantly; the cell's integrity was not compromised. However, since the microchamber technique did not measure membrane currents, selection of short or tall hair

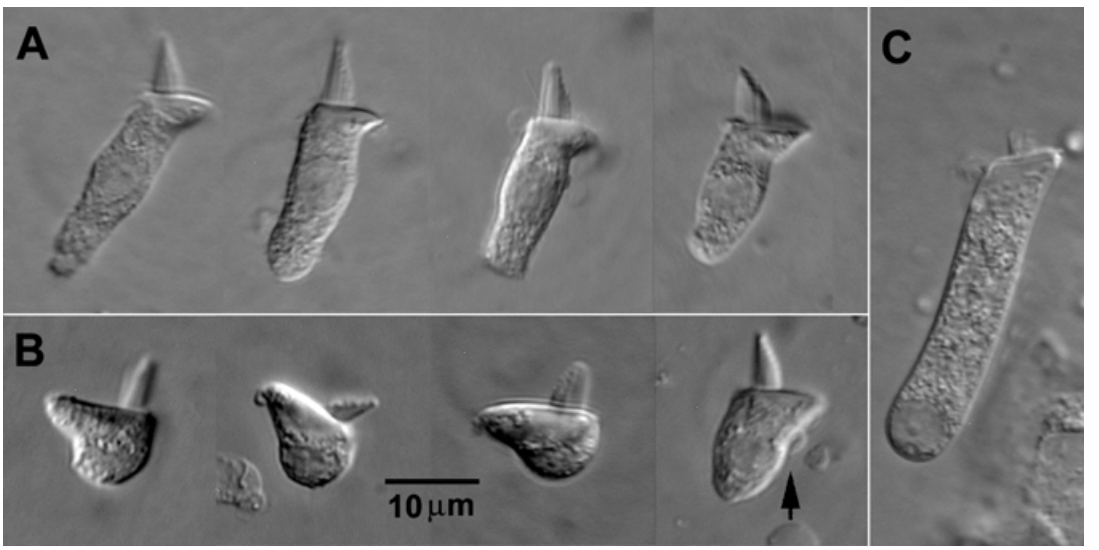

Figure 1. Micrographs of some examples of isolated chick hair cells and a gerbil OHC

A, tall hair cells. *B*, short hair cells. The identity of the cell marked by an arrow is unclear. *C*, an OHC from the apical turn of a gerbil cochlea. All images were captured by a digital camera (Olympus D-490) mounted in a Leica upright microscope with Nomarski optics. Bar represents 10 μm.

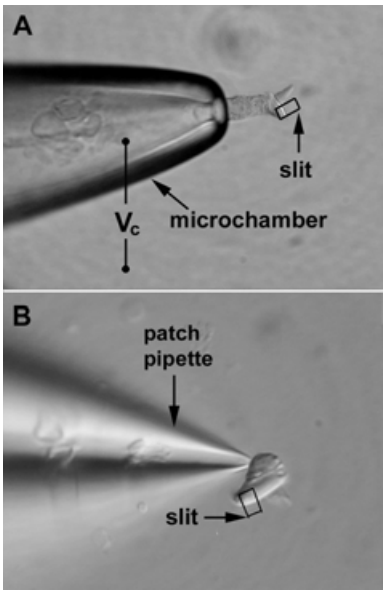

Figure 2. Illustrations of recording somatic motility of chick hair cells with the microchamber and whole-cell voltage-clamp techniques

A, a tall hair cell is partially inserted into the microchamber with its ciliated pole extruded. Command voltage (V_c) is delivered between electrolytes inside and surrounding the microchamber. The partitioning of the cell in the microchamber forms a voltage divider. The voltage drops on the included and excluded membrane segments are of opposite polarity and are estimated based on a simplified model for guinea pig OHCs (Dallos *et al.* 1993). *B*, a short hair cell is under whole-cell voltage-clamp recording. For motility measurement with either technique, a small area on the edge of the cuticular plate is projected onto a photodiode through a rectangular slit in the optical pathway. The photocurrent response is proportional to length changes and is calibrated to length changes by moving the slit to a fixed distance before each trial.

cells for motility measurements was solely based on their appearance. Figure 1 shows some examples of isolated short and tall hair cells to demonstrate their differences in appearance. As shown, THCs are long and cylindrical (Fig. 1*A*), while SHCs are shorter and have wider cuticular surfaces (Fig. 1*B*). These obvious differences made the identification of hair cells fairly straightforward. However, the morphological difference between THCs and SHCs can be less distinct because of a gradual transition in morphology from tall to short hair cells across the width of the basilar papilla. An example of those cells whose identity was equivocal is shown in Fig. 1*B* (marked with an arrow). During motility measurements with the microchamber technique, we normally selected the cells whose morphological features fitted the criteria of 'typical' SHCs or THCs to represent the two hair cell populations. However, motility of those hair cells whose morphology was between short and tall hair cells was also measured to determine whether they were electromotile.

Healthy, solitary hair cells were partially drawn into the microchamber with about 70–80 % of their length extruded (Fig. 2*A*). Cells were identified as healthy if they showed no obvious signs of damage and/or deterioration such as swelling and/or granulation. Transcellular potentials were applied through the microchamber. Length changes of the excluded segment (cuticular plate) were measured. Motile responses were defined as any measurable length change that was repeatable and time-locked to the stimulus. We measured 41 cells that, by definition, were SHCs. Among them, 15 cells were measured by a system that had the ability to resolve motion down to 5 nm. The rest of the cells were measured by a system that had a resolution of 10 nm. The length of the SHCs measured was between 7 and 10 μm with the diameter/length ratio being between 1.1 and 1.4. We also measured 19 THCs (10 cells were measured by the system with 5 nm resolution) whose length varied from 15 to 28 μm. In all 60 (tall and short) cells measured, none

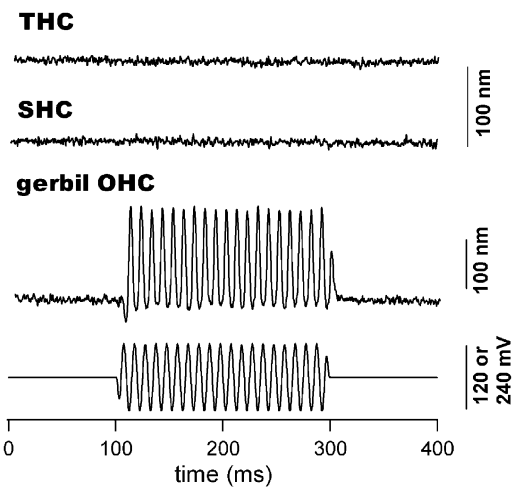

Figure 3. Length change responses measured from isolated chick hair cells and a gerbil OHC

The response was obtained with a photodiode-based motility measurement system after filtering at 200 Hz. Chick hair cells were stimulated with 240 mV (peak-to-peak), 100 Hz sinusoidal voltage burst while 120 mV was applied to the gerbil OHC. The lengths of the short and the tall hair cell shown in this figure were 10 and 26 μm respectively. Both traces are the results of 50 averages. The response from the gerbil OHC was obtained with 5 averages. In all cases, the cells were approximately 70–80 % extruded from the microchamber. The actual voltage received by the extruded segment was estimated to be 48 mV (peak-to-peak) for the chick hair cells. This was based on an extrusion factor of 0.8 (80 %) and a simplified model of the same configuration for guinea pig OHCs (Dallos *et al.* 1993). Based on this estimate, we expected that the voltage received by the chick hair cells under the described experimental condition was much larger than the receptor potential *in vivo*. Note that no motile response was seen in either short or tall hair cells (upper traces). In contrast, robust motility was observed in the gerbil OHC. Cell contraction is plotted upward.

showed any motile responses with 240 mV (peak-to-peak) stimulation. Examples of the lack of motility of tall and short hair cells are shown in Fig. 3. As a positive control, motility of OHCs isolated from adult gerbils was also measured with the same technique. An example of the motile response is depicted in Fig. 3. In the examples, all three cells were stimulated with a 100 Hz voltage burst whose waveform is shown in the bottom panel. As shown, neither THC nor SHC showed any length changes in response to the 240 mV stimulus. In contrast, a robust motile response with both DC and AC components was observed in the gerbil OHC at 120 mV. Motile responses were also examined with sinusoidal voltage bursts of 250 and 1000 Hz in five SHCs and four THCs. No motile response was detected (data not shown). We also measured seven hair cells whose morphological appearance resembled that of the cell shown in Fig. 1*B* (marked by an arrow). None of them exhibited motile responses (data not shown).

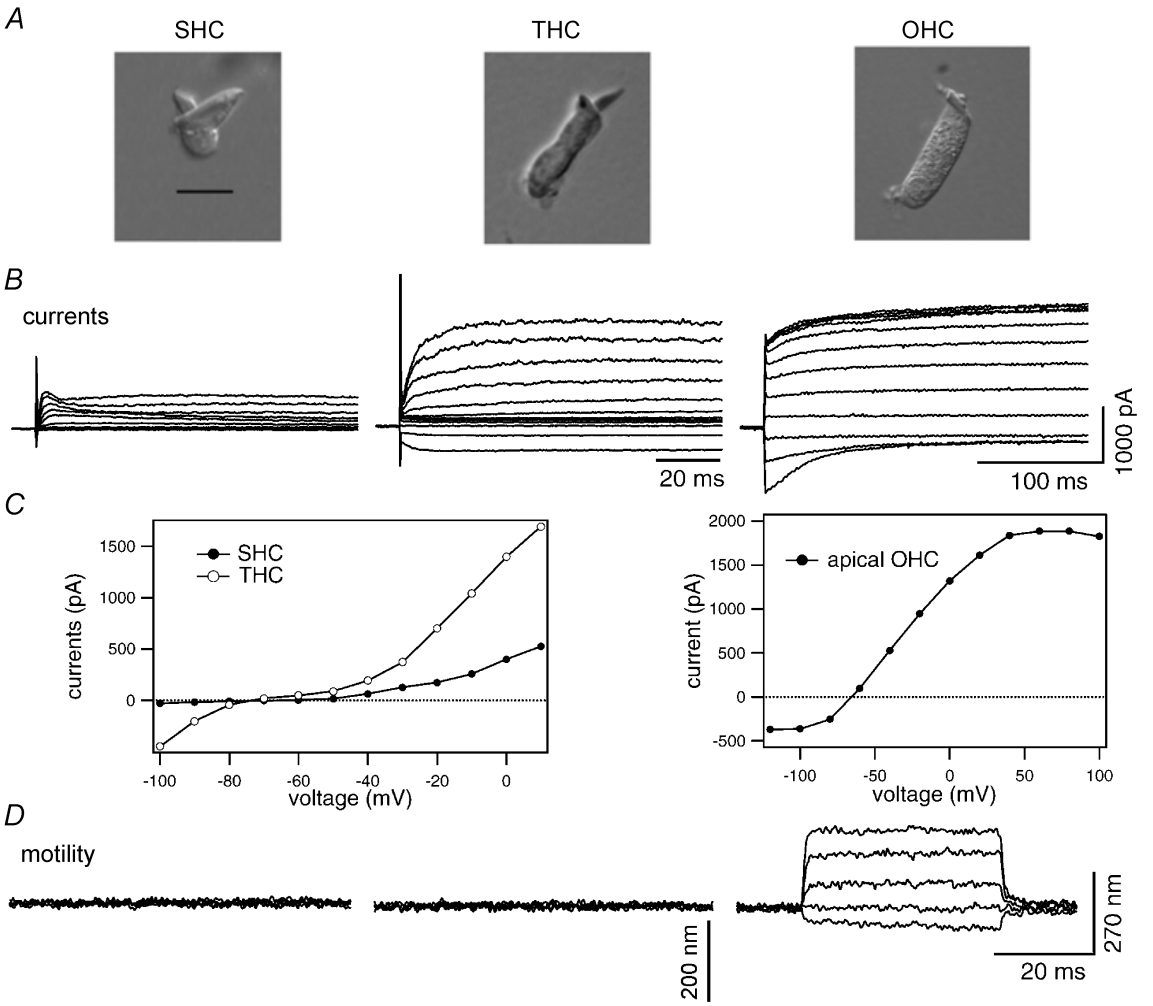

Figure 4. Whole-cell currents and motility measured from chick hair cells and a gerbil OHC

A, images of a SHC, THC and a gerbil OHC. Bar represents 10 μm. To measure whole-cell currents and motility, normal intracellular and extracellular media were used (see Methods). Cells were held at −80 mV for current recordings. Voltage steps (100 ms in duration) varied from −100 to 0 mV in 10 mV steps. The gerbil OHCs were held at −70 mV and voltage steps varied from −120 to 100 mV in 20 mV steps. The currents were filtered at 2 kHz. No averages were used to obtain the current responses (*B*). Series resistance was between 10 and 15 MΩ and was 70–75 % corrected. *C, I–V* curves obtained by measuring from the steady-state responses. The resting membrane potentials (after equilibration with the contents of the patch pipette) were −74 and −65 mV for the tall and short hair cell shown, respectively. The voltage in the *I–V* plots was not corrected for the uncompensated voltage error. The largest voltage error due to the uncompensated series resistance for the SHC was, however, less than 2 mV. *D,* to record motility, all cells were held at −70 mV. Voltage steps (40 ms duration) were varied from −110 to 50 mV in 40 mV steps. The photocurrent responses were filtered at 1000 Hz. The responses obtained from chick hair cells were the results of 50 averages, while the response from the gerbil OHC was obtained with only five averages. Depolarization (or cell contraction) was plotted upwards.

Whole-cell voltage-clamp techniques were also used to obtain whole-cell currents and to evoke length changes. It has been demonstrated that THCs and SHCs possess different membrane conductances. THCs usually produce some combination of delayed rectifier and calcium-activated K^+ currents (Fuchs & Evans, 1990), while SHCs express a rapidly inactivating or 'A-type' current as well as a calcium-activated K^+ current (Murrow & Fuchs, 1990; Murrow, 1994). The voltage-clamp technique allowed us to verify that the selection of SHCs or THCs based on morphological criteria were indeed SHCs or THCs. After the membrane currents were recorded to aid cell identification, motility was measured from these cells. Because the membrane potential was not under direct control with the microchamber technique, the voltage-clamp technique could help to assure that somatic motility, if any, was not overlooked due to the unknown membrane voltage with the microchamber technique.

Whole-cell currents and motile responses were recorded from SHCs and THCs. For comparison, the responses from gerbil OHCs were also recorded. To record currents, the chick hair cells were all held at −80 mV in order to prevent inactivation of the 'A-type' current of SHCs (Murrow & Fuchs, 1990; Murrow, 1994). Voltage steps (100 ms in duration) from −100 mV to 10 mV were delivered. We did not use any channel antagonists in the medium to isolate different currents. However, the differences in current size and response characteristics (activation kinetics) between the two types of cells are apparent, as shown in Fig. 4. All SHCs recorded expressed a combination of a rapidly inactivating or 'A-type' currents and a Ca^{2+} -activated K^+ current. The 'A-type' current was similar to that reported by Murrow & Fuchs (1990) and Murrow (1994) after the Ca^{2+}-activated K^+ currents were subtracted out (using a holding potential of −40 mV, where 'A-type' current was inactivated). In contrast, THCs expressed some combination of delayed rectifier and Ca^{2+}-activated K^+ current. An inwardly rectifying current was also seen in some THCs (such as the one shown in Fig. 4). Examples of whole-cell currents recorded from a short and tall hair cell are shown in Fig. 4*B*. *I–V* curves measured from the steady-state

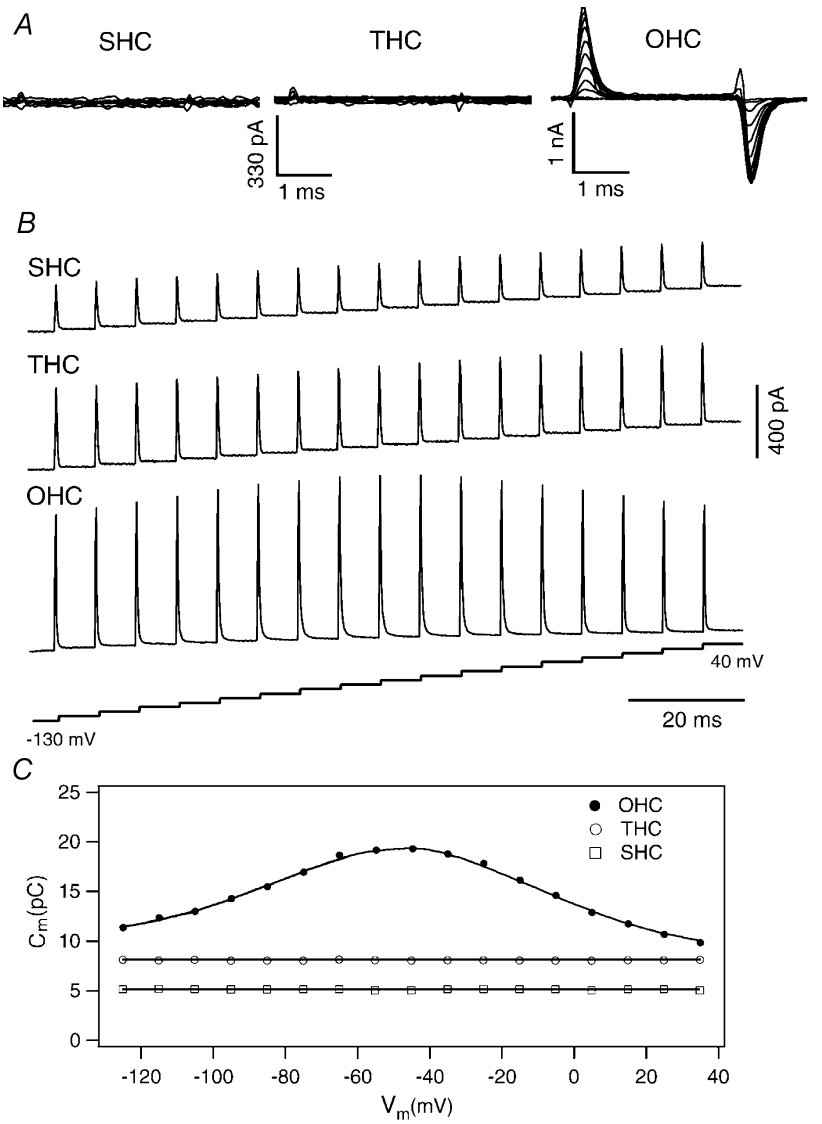

Figure 5. Non-linear capacitive currents obtained from chick hair cells and a gerbil OHC

Ionic currents were blocked during recordings (see Methods). *A*, non-linear capacitive currents obtained by *P*/−4 procedure at a holding and subtracting potential of −120 mV. Voltage steps were 5 ms in duration and 20 mV increments up to 40 mV. The capacitive currents shown were the results of three averages. Note that only the gerbil OHC expresses the transient capacitive current after the linear capacitive component was subtracted out. *B*, non-linear capacitive currents obtained by stair voltage protocol (from −130 mV to 40 mV in 10 mV steps) from a holding potential of −70 mV. Note that short or tall hair cells only express linear transient capacitive current while non-linear transient capacitive current is seen in the gerbil OHC. *C*, the non-linear capacitance of the gerbil OHC as a function of voltage is fitted by the first derivative of a two-state Boltzmann function with Q_{max}, $V_{1/2}$ and C_m of 2.8 pC, −43.3 mV and 8.5 pF respectively.

responses are also plotted (Fig. 4*C*). Motility was measured from those cells after their identity was established (Fig. 4*D*). We measured eight SHCs and five THCs with the system that had a resolution of 5 nm. The cells were held at −70 mV and voltage steps (40 ms in duration) from −110 to 50 in 40 mV steps were applied to the cells. None of the cells showed any motile responses. Examples of the lack of response are given in Fig. 4*D*. We also stimulated four SHCs and three THCs with current injection (from −0.2 to 1.2 nA in 0.2 nA steps) under the whole-cell current-clamp condition. No motility was observed. For control purpose, five OHCs isolated from gerbil cochleae were also measured. Robust motile responses were observed in all cells measured when their membrane potential was stepped from −110 to 50 mV in 40 mV steps. An example of the motile response is shown in Fig. 4*D*.

Measurements of voltage-dependent non-linear capacitance

Associated with the OHC electromotility is an electrical signature, a voltage-dependent capacitance or, correspondingly, a gating charge movement (Ashmore, 1989; Santos-Sacchi, 1991), similar to the gating currents of voltage-gated ion channels (Armstrong & Bezanilla, 1973). The gating currents are thought to arise from a redistribution of charged voltage sensors across the membrane. In OHCs, the non-linear capacitance is a function of membrane potential with a peak between −70 and −20 mV (Santos-Sacchi, 1991). Non-linear capacitance has generally served as an assay to reflect electromotility (Santos-Sacchi, 1991; Gale & Ashmore, 1997*a*; Zheng *et al.* 2000). The charge movement has also been measured from membrane patches from OHCs (Gale & Ashmore, 1997*b*) and from prestin-transfected heterologous cells (Oliver *et al.* 2001). Since non-linear capacitance can be measured from only a small number of motor proteins on the membrane patches, such measurement should be sensitive enough to detect charge movements in whole cells if chick hair cells possessed a voltage-gated motor protein such as prestin found in OHCs (Zheng *et al.* 2000). We measured the non-linear capacitive current from chick hair cells to complement the motility measurement with the photodiode technique. More importantly, because of its high sensitivity, this technique was used to verify that no small prestin-based motile response had been missed due to the detection limit of 5 nm of our measurement system.

Voltage-dependent charge movement (non-linear capacitive current) was measured from seven SHCs and four THCs from four cochleae, using a standard subtraction protocol after blocking ionic currents (see Methods). For control purposes, non-linear capacitive current was also measured from gerbil OHCs. The cells were held and subtracted at −120 mV and voltage steps of 10 ms duration varied between −120 and 10 mV. Examples of such measurements obtained from a representative SHC, THC and gerbil OHC are shown in Fig. 5*A*. As shown, no measurable non-linear capacitive current was observed from either SHCs or THCs. In contrast, the gerbil OHC displayed transient capacitive currents.

Non-linear capacitance was also measured using a voltage stair protocol (Huang & Santos-Sacchi, 1993). The cells were stimulated with stair voltage commands between −130 mV and +40 mV in increments of 10 mV from a holding potential of −70 mV. We measured six SHCs and five THCs isolated from four cochleae with this protocol. Examples of the recordings are shown in Fig. 5*B*. It is apparent from the figure that SHCs or THCs only express linear transient capacitive current. In contrast, non-linear transient capacitive currents were seen in gerbil OHCs. We measured eight OHCs from four gerbil cochleae. In those eight cells measured, the non-linear capacitance peaked between −22 and −85 mV, asymptoting to the linear capacitance of the cells at both large negative and positive membrane potential. An example of the capacitive current trace, and the calculated non-linear capacitance as a function of voltage is given in Fig. 5*B*.

DISCUSSION

By analogy with mammalian OHCs, it is speculated that chick SHCs perform a motor function supplying energy tuned into the vibration of the cochlear partition (for review see Fettiplace & Fuchs, 1999). The specific source of this electromotile process could conceivably reside in the stereocilia bundle and/or the soma involving a motor protein similar to prestin (Zheng *et al.* 2000). With a sensitive motility measurement system, we have demonstrated here that neither SHCs nor THCs possess voltage-dependent somatic motility. Furthermore, SHCs and THCs did not exhibit voltage-dependent non-linear capacitance, consistent with their lack of somatic motility. The negative results were apparently not due to lack of sensitivity of our measurement system. In mammalian OHCs, the maximal motile response was of the order of a few hundred nanometres to a few micrometres, or 2–5 % of the resting cell length when the cells were stimulated with a large voltage command (Brownell *et al.* 1985; Ashmore, 1987; Santos-Sacchi, 1989). Accordingly, we would assume that if SHCs were motile, the maximal response would be in the range of 140 nm (assuming a 2 % length change of a 7 μm SHC), well above the 5 nm sensitivity of our measurement system. The lack of non-linear capacitance also suggests there are no prestin-based motor proteins in SHCs and THCs. Collectively, these results suggest that chick SHCs or THCs do not possess voltage-dependent somatic motility. The lack of an electromotile response in chick hair cells strongly suggests that reverse transduction in chick hair cells is not generated by somatic motility.

It has recently been shown that transmembrane voltage can modulate membrane tension and that it can induce movement in kidney cells with no membrane-bound motor proteins (Zhang *et al.* 2001). Such movement, as expected from thermodynamics, was rather small, of an order of 1 nm per 100 mV. While we cannot completely rule out similar movement that was below the resolution of our system (5 nm) in hair cells, such movements are probably too small and too insensitive to the membrane potential changes to provide the power for the cochlear amplifier. In addition, hair cells and supporting cells in the avian cochlea are tightly packed with no extracellular space. Thus, even if they produced very small movements, morphological contraints of surrounding cells could render any small motion completely ineffective. We want to point out that although OHC motility around the threshold is also believed to be small in the mammalian cochlea, its sensitivity, however, is of an order of 5–25 nm mV^{-1}.

While Brix & Manley (1994) were examining bundle motions in chick hair cells, they also examined somatic motility in chick hair cells. In their study, currents were injected by microelectrodes and length changes were measured by videomicroscopy, which had a resolution of 76 nm and a frequency limit of less than 30 Hz. Contrary to our findings, contractions of the order of 3 % of the total resting cell length were reported. Assuming that the length of chick hair cells varies from 7 to 30 μm, a 3 % length change would result in a motion of 210 to 900 nm, well above the 5 nm sensitivity of our measurement system. Their results are difficult to reconcile with our results since we did not observe any motile response with either voltage stimulation or current injections in both THCs and SHCs. It is interesting to note that one recent study (Köppl *et al.* 2002) using freeze-fracture technique demonstrated that the density of membrane particles in bird hair cells was approximately 1890 μm^{-2}, similar to that seen in inner hair cells (IHCs). While the size of the particles (~10 nm) in bird hair cells was comparable to that of OHCs and IHCs, the density was substantially less than ~5100 particles per square micron normally seen in mammalian OHCs (Forge, 1991). This suggests that bird hair cells do not have membrane-bound motility motors consistent with those seen in OHC (Köppl *et al.* 2002).

We did not attempt to examine bundle movements in this study; however, small hair bundle movements, with a sensitivity of 0.6 nm mV^{-1}, have been observed in chicken hair cells (Brix & Manley, 1994). The bundle movements, which changed direction with current polarity, were hypothesized to arise from the adaptation motor in the bundle. More recently, spontaneous as well as evoked damped oscillatory bundle movements have been observed in chick SHCs (Hudspeth *et al.* 2000). The active mechanical response in chick SHCs resembles those recorded from hair cells of the turtle's cochlea and the frog's sacculus, but is several-fold larger and occurs at a frequency of 235 Hz, much higher than that of spontaneous oscillations observed in hair cells of the turtle's cochlea and the frog's sacculus. In bullfrog saccular hair cells, stimulus-induced deflections of the bundle resulted in a biphasic response; the initial response occurred in same direction as the stimulus and was followed a few milliseconds later by movement in the opposite direction (Benser *et al.* 1996). Bundle movements were sometimes accompanied by a damped oscillation. Saccular hair cells also produce spontaneous oscillations in the 5–40 Hz range when the apical pole of the hair cell is bathed in an endolymph-like solution (Martin & Hudspeth, 1999). Moreover, small external stimuli applied to the bundle with a glass rod evoked bundle movements larger than the original stimulus, indicating that the bundles were providing energy to enhance their movement and overcome the viscous fluid drag of the endolymph. These results suggest that the electrically evoked emissions seen in non-mammalian ears may arise from voltage-dependent oscillations in the stereocilia bundles.

The lack of somatic motility in chick hair cells leads to the alternative hypothesis that the active process resides in the stereocilia bundle in birds. This interpretation, however, does not necessarily imply that hair-bundle motility also underlies cochlear amplification in mammalian hair cells. OHC motility (Brownell *et al.* 1985), accompanied by somatic stiffness change (He & Dallos, 1999), remains the most plausible candidate accounting for cochlear amplification, since neither spontaneous nor evoked hair bundle motility has been reported in mammalian hair cells (for review see Fettiplace *et al.* 2001). Nevertheless, recordings in neonatal mouse preparations have shown that the mechanotransducer currents in cultured hair cells possess some properties similar to those seen in lower vertebrates, and exhibit both gating compliance (Russell *et al.* 1992; van Netten & Kros, 2000) and some adaptation (Kros *et al.* 1992). Although an amplificatory mechanism based on a collective action of motors in the soma and the hair bundle cannot be completely ruled out in the mammalian OHCs, overwhelming evidence indicates that the basis of cochlear amplification in mammals is a voltage-dependent somatic length change of OHCs (Liberman *et al.* 2002). Therefore, it is very likely that mammals and non-mammals use different mechanisms for cochlear amplification and frequency discrimination.

REFERENCES

Armstrong CM & Bezanilla F (1973). Currents related to movement of the gating particles of the sodium channels. *Nature* **242**, 459–461.

Ashmore JF (1987). A fast motile response in guinea-pig outer hair cells: the cellular basis of the cochlear amplifier. *J Physiol* **388**, 323–347.

Ashmore JF (1989). Transducer motor coupling in cochlear outer hair cells. In *Cochlear Mechanisms*, ed. Wilson JP & Kemp DT, pp. 107–116. Plenum Press, London.

Benser ME, Marquis RE & Hudspeth AJ (1996). Rapid, active hair bundle movements in hair cells from the bullfrog's sacculus. *J Neurosci* **16**, 5629–5643.

Bezanilla F & Armstrong CM (1977). Inactivation of the sodium channels. I. Sodium currents experiments. *J Gen Physiol* **70**, 549–566.

Brix J & Manley GA (1994). Mechanical and electromechanical properties of the stereovillar bundles of isolated and cultured hair cells of the chicken. *Hear Res* **76**, 147–157.

Brownell WE (1990). Outer hair cell electromotility and otoacoustic emissions. *Ear Hear* **11**, 82–92.

Brownell WE, Bader CR, Bertrand D & de Ribaupierre Y (1985). Evoked mechanical responses of isolated cochlear outer hair cells. *Science* **227**, 194–196.

Chen L, Sun W & Salvi RJ (2001). Electrically-evoked otoacoustic emissions from the chicken ear. *Hear Res* **161**, 54–64.

Chen L, Trautwein P, Shero M & Salvi RJ (1996). Correlation of hair cell regeneration with physiology and psychophysics in adult chickens following acoustic trauma. In *Auditory System Plasticity and Regeneration*, ed. Salvi RJ, Henderson D, Fiorino F & Colletti V, pp. 43–61. Thieme Medical Publishers, New York.

Crawford AC & Fettiplace R (1985). The mechanical properties of ciliary bundles of turtle cochlear hair cells. *J Physiol* **364**, 359–379.

Dallos P (1996). Overview: Cochlear neurobiology. In *The Cochlea* ed. Dallos P, Popper AN & Fay RR, pp. 1–43. Springer-Verlag, New York.

Dallos P, Evans BN & Hallworth R (1991). Nature of the motor element in electrokinetic shape changes of cochlear outer hair cells. *Nature* **350**, 155–157.

Dallos P, Hallworth R & Evans BN (1993). Theory of electrically driven shape changes of cochlear outer hair cells. *J Neurophysiol* **70**, 299–323.

Evans BN, Hallworth R & Dallos P (1991). Outer hair cell electromotility: the sensitivity and vulnerability of the DC component. *Hear Res* **52**, 288–304.

Fettiplace R & Fuchs PA (1999). Mechanisms of hair cell tuning. *Annu Rev Physiol* **61**, 809–834.

Fettiplace R, Ricci AJ & Hackney CM (2001). Clues to the cochlear amplifier from the turtle ear. *Trends Neurosci* **24**, 169–175.

Fischer FP (1994). General pattern and morphological specializations of the avian cochlea. *Scanning Microsc* **8**, 351–364.

Forge A (1991). Structural features of the lateral walls in mammalian cochlear outer hair cells. *Cell Tissue Res* **265**, 473–483.

Fuchs PA (1992). Ionic currents in cochlear hair cells. *Prog Neurobiol* **39**, 493–505.

Fuchs PA & Evans MG (1990). Potassium currents in hair cells isolated from the cochlea of the chick. *J Physiol* **429**, 529–551.

Fuchs PA, Nagai T & Evans MG (1988). Electrical tuning in hair cells isolated from the chick cochlea. *J Neurosci* **8**, 2460–2467.

Gale JE & Ashmore JF (1997*a*). An intrinsic frequency limit to the cochlear amplifier. *Nature* **389**, 63–66.

Gale JE & Ashmore JF (1997*b*). The outer hair cell motor in membrane patches. *Pflügers Arch* **434**, 267–271.

He DZZ & Dallos P (1999). Somatic stiffness of cochlear outer hair cells is voltage-dependent. *Proc Natl Acad Sci U S A* **96**, 8223–8228.

He DZZ, Evans BN & Dallos P (1994). First appearance and development of electromotility in neonatal gerbil outer hair cells. *Hear Res* **78**, 77–90.

Holley MC & Ashmore JF (1988). On the mechanism of a high-frequency force generator in outer hair cells isolated from the guinea pig cochlea. *Proc R Soc Lond* B *Biol Sci* **232**, 413–429.

Howard J & Hudspeth AJ (1987). Mechanical relaxation of the hair bundle mediates adaptation in mechanoelectrical transduction by the bullfrog's saccular hair cell. *Proc Natl Acad Sci U S A* **84**, 3064–3068.

Huang G & Santos-sacchi J (1993). Mapping the distribution of the outer hair cell motility voltage sensor by electrical amputation. *Biophys J* **65**, 2228–2236.

Hudspeth AJ (1997). Mechanical amplification of stimuli by hair cells. *Curr Opin Neurobiol* **7**, 480–486.

Hudspeth AJ, Choe Y, Mehta AD & Martin P (2000). Putting ion channels to work: mechanoelectrical transduction, adaptation, and amplification by hair cells. *Proc Natl Acad Sci U S A* **97**, 11765–11772.

Iwasa KH (1994). A membrane motor model for the fast motility of the outer hair cells. *J Acoust Soc Am* **96**, 2216–2224.

Köpple C, Forge A & Manley GA (2002). No correlates for somatic motility in freeze-fractured hair-cell membranes of lizards and birds. In *Biophysics of the Cochlea: From Molecule to Model*, pp. 410–411. Titisee, Germany.

Kros CJ, Rüsch A & Richardson GP (1992). Mechanoelectrical transducer currents in hair cells of the cultured neonatal mouse cochlea. *Proc R Soc Lond* B *Biol Sci* **249**, 185–193.

Liberman MC, Gao JG, He DZZ, Wu XD, Jia SP & Zuo J (2002). Prestin is required for electromotility of the outer hair cell and for the cochlear amplifier. *Nature* **419**, 300–304.

Manley GA, Kirk DL, Köppl C & Yates GK (2000). Cochlear mechanisms from a phylogenetic viewpoint. *Proc Natl Acad Sci U S A* **97**, 11736–11743.

Manley GA, Kirk DL, Köppl C & Yates GK (2001). *In vivo* evidence for a cochlear amplifier in the hair-cell bundle of lizards. *Proc Natl Acad Sci U S A* **98**, 2826–2831.

Martin P & Hudspeth AJ (1999). Active hair-bundle movements can amplify a hair cell's response to oscillatory mechanical stimuli. *Proc Natl Acad Sci U S A* **96**, 14306–14311.

Murrow BW (1994). Position-dependent expression of potassium currents by chick cochlear hair cells. *J Physiol* **480**, 247–259.

Murrow BW & Fuchs PA (1990). Preferential expression of transient potassium current (IA) by 'short' hair cells of the chick's cochlea. *Proc R Soc Lond* B *Biol Sci* **242**, 189–195.

Oliver D, He DZZ, Klocker N, Ludwig J, Schulte U, Waldegger S, Ruppersberg JP, Dallos P & Fakler B (2001). Intracellular anions as the voltage sensor of prestin, the outer hair cell motor protein. *Science* **292**, 2340–2343.

Ricci AJ, Crawford AC & Fettiplace R (2000). Active hair bundle motion linked to fast transducer adaptation in auditory hair cells. *J Neurosci* **20**, 7131–7142.

Ricci AJ, Crawford AC & Fettiplace R (2002). Mechanisms of active hair bundle motion in auditory hair cells. *J Neurosci* **22**, 44–52.

Russell IJ, Kossl M & Richardson GP (1992). Nonlinear mechanical responses of mouse cochlear hair bundles. *Proc R Soc B Lond B Biol Sci* **250**, 217–227.

Santos-Sacchi J (1989). Asymmetry in voltage-dependent movements of isolated outer hair cells from the organ of Corti. *J Neurosci* **9**, 2954–2962.

Santos-Sacchi J (1991). Reversible inhibition of voltage-dependent outer hair cell motility and capacitance. *J Neurosci* **11**, 3096–3110.

Tanaka K & Smith C (1978). Structure of the chicken's inner ear: SEM and TEM study. *Am J Anat* **153**, 251–272.

van Netten SM & Kros CJ (2000). Gating energies and forces of the mammalian hair cell transducer channel and related hair bundle mechanics. *Proc R Soc Lond* B *Biol Sci* **267**, 1915–1923.

Wit HP, van Dijk P & Segenhout JM (1989). DC injection alters spontaneous otoacoustic emission frequency in the frog. *Hear Res* **41**, 199–204.

Zhang PC, Keleshian AM & Sachs F (2001). Voltage-induced membrane movement. *Nature* **413**, 428–432.

Zheng J, Shen WX, He DZZ, Long K, Madison LD & Dallos P (2000). Prestin is the motor protein of cochlear outer hair cells. *Nature* **405**, 149–155.

Acknowledgements

This work has been supported by NIH grants R01 DC 04696 to D.H., R01 DC 04279 to K.B. and R01 DC 01685 and P01 DC03600–01A1 to R.S. from the National Institute of Deafness and Other Communication Disorders. We want to thank L. Reiss for machine shop work and D. Fitzpatrick for electronic support.